

## EXPERIMENTAL INVESTIGATION OF HEAT PIPE THERMAL PERFORMANCE WITH MICROGROOVES FABRICATED BY WIRE ELECTRICAL DISCHARGE MACHINING

by

**Felipe BAPTISTA NISHIDA<sup>a</sup>, Larissa KRAMBECK<sup>a</sup>,  
Paulo Henrique DIAS DOS SANTOS<sup>b</sup>, and Thiago ANTONINI ALVES<sup>a\*</sup>**

<sup>a</sup> Federal University of Technology – Parana (UTFPR), Ponta Grossa, Brazil

<sup>b</sup> Federal University of Technology – Parana (UTFPR), Curitiba, Brazil

Original scientific paper

<https://doi.org/10.2298/TSCI180227206B>

*This work presents the use of electrical discharge machining (EDM) technology for manufacturing of three different types of axial microgrooves in heat pipes. This specific process, called wire electrical discharge machining (wire-EDM), allows the fabrication of microgrooves on the inner wall of a heat pipe with accuracy. Different from other capillary structures, such as composite wick and screen mesh, the material is removed from the pipe's container in order to conceive the capillary structure, which contributes with the mass reduction of the passive two-phase heat transfer device. The heat pipes were manufactured from a straight copper pipe with the external diameter of 9.45 mm, the inner diameter of 6.20 mm, and a total length of 200 mm. Three types of axial microgrooves were manufactured for constant width (35  $\mu\text{m}$ ) and varying the depth (from 30-48  $\mu\text{m}$ ), and thickness (from 35-70  $\mu\text{m}$ ). The number of microgrooves was also varied from 21-32 microgrooves. Water was used as the working fluid and the loading filling ratio was 60% of the evaporator volume. The condenser was cooled by air forced convection, the adiabatic section was insulated and the evaporator was heated by an electrical resistor and it was insulated from the environment with aeronautic thermal insulation. The thermal performance of the heat pipes are analyzed based on experimental results, so the heat pipes were tested at the horizontal and different inclinations under different low heat loads (from 5-50 W or a heat flux from 0.21-2.10 W/cm<sup>2</sup>). The experimental results showed that the axial microgrooves manufactured by the wire-EDM process worked satisfactorily in all analyzed cases and microgrooves of Type 1 showed a better thermal performance when compared with the others.*

Key words: *heat pipe, axial microgrooves, wire-EDM, electrical discharge machining*

### Introduction

Heat pipes are passive devices used to improve heat transfer in many industrial fields such as electronics, telecommunications, aerospace, among others. The heat transmitted through these devices is based on phase change [1]. They became very popular because of their effectiveness and convenience. Major advantages of heat pipes include a very high thermal conductance, no pumping power requirements, no moving parts, and relatively low pressure drops [2]. Details on the operating principle of the heat pipes can be found in [3-6].

\* Corresponding author, e-mail: thiagoalves@utfpr.edu.br

The heat pipes basically consist of a metal tube sealed with capillary structure internally, which is embedded with a working fluid. There are several kinds of capillary structures for heat pipes, as sintered, grooved, screened mesh, and composited [7]. Different from other capillary structures, in the axial microgrooves, the material is removed from the pipe's container in order to conceive the capillary structure, which contributes with the mass reduction of the passive two-phase heat transfer device [8].

However, grooved heat pipes are limited by conventional fabrication techniques, for instance, milling, broaching or ploughing [9]. It is a challenging task to conceive a capillary structure with small pores making use of such conventional methods, therefore, an axial grooved heat pipe fabricated through conventional ways, is likely to have a low capillary pressure, as well as a smaller heat transfer capacity. Many researchers applied ideas of new configuration projects and new fabrication processes for capillary structures, willing to increase the capillary force and the heat transfer capacity [10]. At the present time, more advanced fabrication approaches have been used, for example, the electrical discharge machining and chemical etching of metals, that made possible the manufacture of triangular, trapezoidal, synodical, and rectangular grooves [11, 12].

Then, the main issue is to reduce the geometry of the capillary structures; hence, new fabrication techniques for axial microgrooves in heat pipes are of great importance [13]. Some papers available in the literature, [9-11] and [14-17], have in common the question of the search for new methods in the process of microgrooves manufacturing in heat pipes, aiming the optimization of its operation. The improvement of the pore size for an increase of the capillary force, the reduction of the device mass, the facility and manufacturing cost and/or the type of application can be ways to optimize [13].

In this context, this work presents the use of EDM technology for manufacturing of three different types of axial microgrooves in heat pipes. This specific process, called wire-EDM, allows the fabrication of microgrooves on the inner wall of a heat pipe with accuracy. It presents discussions on the thermal performance of heat pipe fabricated based on experimental results. The heat pipes analyzed were tested at the horizontal and different inclinations ( $+45^\circ$ ,  $+90^\circ$ ,  $-45^\circ$ , and  $-90^\circ$ ) under different low heat loads (from 5 up to 50 W or a heat flux from 0.21-2.10 W/cm<sup>2</sup>).

### Wire-EDM zechnology

The wire-EDM works by means of an electrode wire passing through the workpiece, fig. 1. The wire is precisely monitored by a system of computer numerical control. Like any

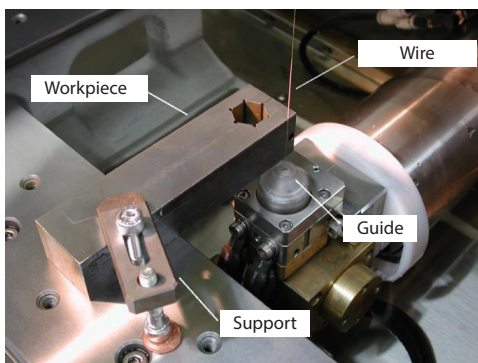


Figure 1. Wire-EDM [18]

other machining tool, the wire-EDM removes material, but with electricity through erosion by a spark. Therefore, the material to be worked on must be electrically conductive. Fast electrical pulses of direct current are generated between the electrode wire and the workpiece. When a high voltage is applied, the fluid ionized, then a precisely controlled spark burns a small section of the workpiece, causing the melt and vaporization of the material. These electrical pulses are repeated thousands of times per second. The pressurized cooling fluid, the dielectric fluid, cools the vaporized metal and forces the solid-

ified particles out of the cut region. The dielectric fluid passes through a filter that removes the solid particles. To maintain the accuracy of the machine, the dielectric fluid-flows through a thermostated bath that keeps the liquid at constant temperature [19]. With the wire-EDM technology, complex cuts can be run on difficult-to-machine metals without the need for expensive precision milling [20].

**The capillary structure**

The microgrooves were made in a straight copper tube by wire-EDM process. Three types of axial microgrooves were manufactured for constant width 35 μm, and varying the depth from 30-48 μm, and thickness, from 35-70 μm. The number of microgrooves was also varied from 21 up to 32 grooves. Figure 2 presents a schematic diagram of the microgroove geometric configuration and tab. 1 shows the characteristics of the microgrooves. The SEM micrographs of the microgrooves are shown in fig. 3.

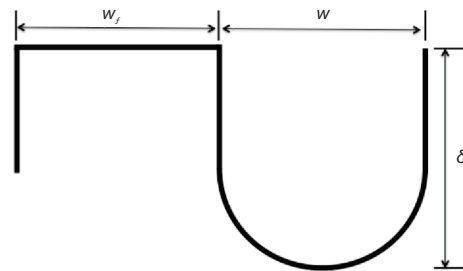


**Figure 2. Schematic diagram of the microgroove geometric configuration**

**Table 1. Characteristics of microgrooves**

Characteristics	Symbol	Type #1	Type #2	Type #3
Microgroove depth [m]	$\delta$	1.2 $\phi$ (30 μm)	1.9 $\phi$ (48 μm)	1.2 $\phi$ (30 μm)
Microgroove width [m]	$w$	1.4 $\phi$ (35 μm)	1.4 $\phi$ (35 μm)	1.4 $\phi$ (35 μm)
Microgroove thickness [m]	$w_f$	1.4 $\phi$ (35 μm)	1.4 $\phi$ (35 μm)	2.8 $\phi$ (70 μm)
Number of microgrooves	$N$	32	32	21

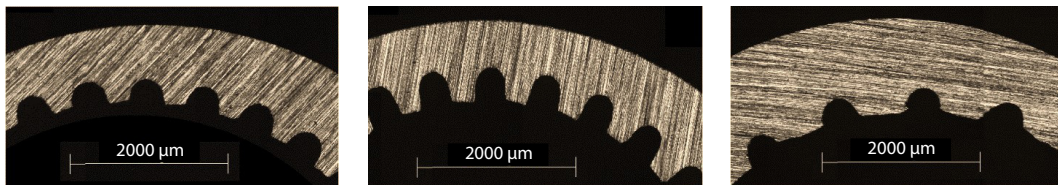


**Figure 3. The SEM micrographs of the microgrooves; (a) type 1, (b) type 2, and (c) type 3**

**The developed heat pipes**

The methodology for manufacturing, tests, and thermal analysis of the heat pipes was developed based on considerations of [7, 8, 13, 21, 22]. Three heat pipes were produced from the grooved copper tubes ASTM B-75 alloy 122 with an outer diameter of 9.45 mm, an inner diameter of 6.20 mm, and a length of 200 mm. The heat pipes have an evaporator region with 80 mm in length, an adiabatic region of 20 mm in length, and a condensation region with 100 mm in length. Due to these geometric characteristics, the heat pipes can be used in the thermal management of electronic equipment. Water was used as the working fluid and the loading filling ratio was 60% of the evaporator volume. Table 2 shows the main characteristics of heat pipes analyzed in this work.

**Table 2. Main characteristics of heat pipes**

Characteristics	Type 1	Type 2	Type 3
Inner diameter [mm]	6.20	6.20	6.20
Outer diameter [mm]	9.45	9.45	9.45
Evaporator length [mm]	80.0	80.0	80.0
Adiabatic section length [mm]	20.0	20.0	20.0
Condenser length [mm]	100	100	100
Working fluid	Water	Water	Water
Filling ratio [%]	60	60	60
Volume of working fluid [mL]	1.80	1.70	1.60
Number of microgrooves	32	32	21

## Experimental analysis

### Experimental apparatus

The experimental apparatus used for the experimental tests, shown in fig. 4(a), is composed of a power supply unit Agilent™ U8002A, a data logger Agilent™ 34970A with 20 channels, a laptop Dell™, a uninterruptible power supply NHS™, a universal support, and a fan Ultrar™. An schematic diagram of the experimental apparatus including the size of the fan and its distance from the heat pipe is shown in fig. 4(b).

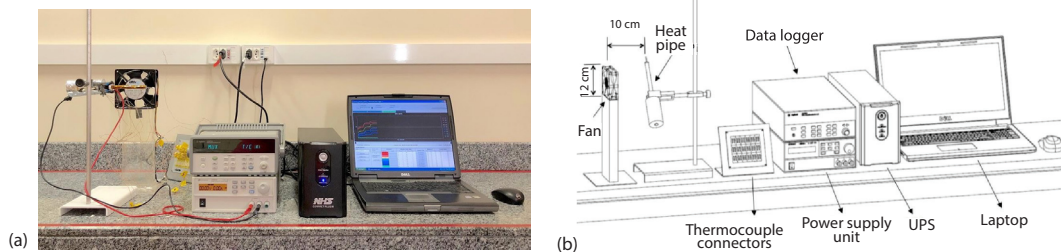


**Figure 4. Experimental apparatus; (a) photograph, (b) schematic diagram**

For the evaluation of the thermal performance of the heat pipes, *K*-type thermocouples Omega Engineering™ were used. They were fixed on the outer surface of heat pipes by a thermosensitive adhesive strip Kapton™. As shown in fig. 5, there were three thermocouples in the evaporator ( $T_{\text{evap},1}$ ,  $T_{\text{evap},2}$ , and  $T_{\text{evap},3}$ ), one thermocouple in the adiabatic section ( $T_{\text{adiab}}$ ), and four thermocouples in the condenser ( $T_{\text{cond},1}$ ,  $T_{\text{cond},2}$ ,  $T_{\text{cond},3}$ , and  $T_{\text{cond},4}$ ) in heat pipes.

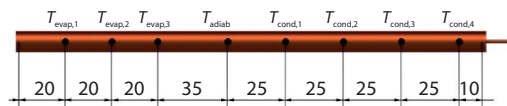


**Figure 5. Thermocouple positions [mm]**

The condenser was cooled by air forced convection. The adiabatic section was insulated with fiberglass tape Omega Engineering™. The evaporator was heated by a strip electrical resistor Omega Engineering™ (nickel-chrome alloy) with 0.1 mm of thickness and 3.5 mm of width and, also, was insulated from the environment with aeronautic thermal insulation MTI Polyfab™ and a layer of polyethylene 3M™, ensuring that the generated heat by Joule effect was transmitted to the evaporator. The evaporator insulation has a total thickness of 14.5 mm calculated from the definition of the critical radius of insulation for a cylindrical body,

considering the thermal conductivity of the insulation and the external convection heat transfer coefficient.

### Experimental procedure

To ensure the best results and the repeatability of experimental tests, the environment temperature was maintained at  $20\text{ }^{\circ}\text{C} \pm 1\text{ }^{\circ}\text{C}$  by the thermal conditioning system Carrier<sup>TM</sup>. The relative humidity varied from 60-70% and have no effect in any experimental result. The heat pipes were tested at the horizontal and different inclinations ( $+45^{\circ}$ ,  $+90^{\circ}$ ,  $-45^{\circ}$ , and  $-90^{\circ}$ ). Note the angles are in positive value when the heat pipe is in the bottom heat mode and the angles are in negative value when the heat pipe is in the top heat mode. The heat pipe was carefully fixed to the universal support with bracket in the adiabatic region at the operating positions, as shown in fig. 6. The fan was turned on, positioned correctly in the condenser region of the heat pipe and set at an average air velocity of 5 m/s controlled by a calibrated potentiometer and an anemometer with a combined error of  $\pm 0.2$  m/s. The average air velocity was calculated in accordance to the American Society of Heating, Refrigerating and Air-Conditioning Engineers (ASHRAE) Handbook [23]. The data logger was turned on, and the temperatures measured by the K-type thermocouples. The temperatures were verified according to the environment temperature, and if these were stable and approximately  $20\text{ }^{\circ}\text{C}$ , finally, the power supply unit was turned on and adjusted to the dissipation power desired.

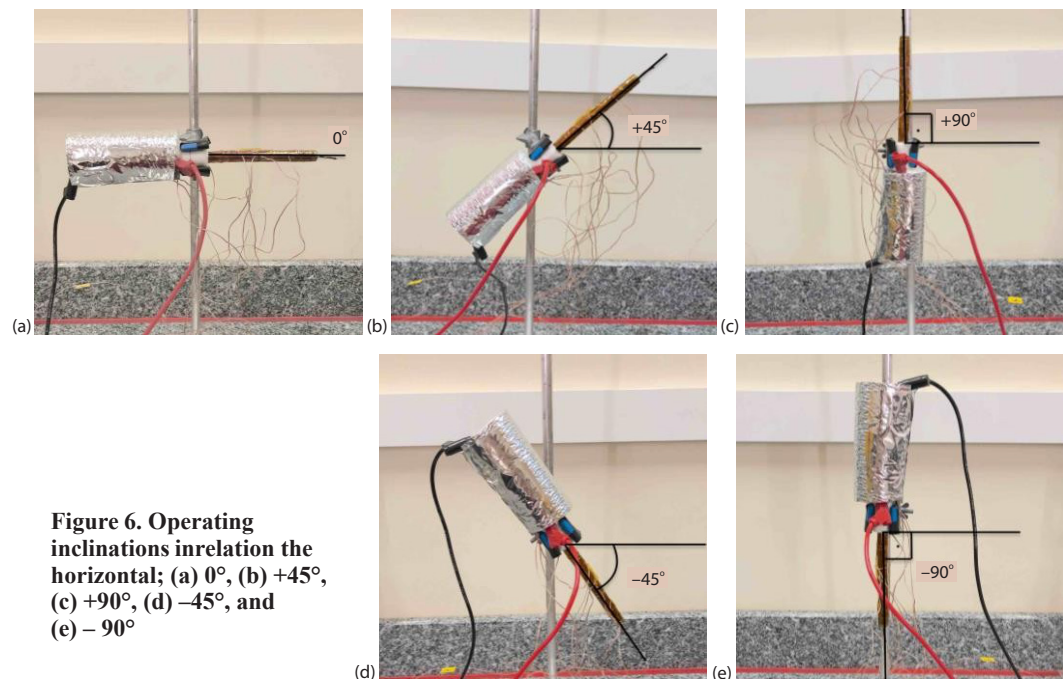


**Figure 6. Operating inclinations in relation the horizontal; (a)  $0^{\circ}$ , (b)  $+45^{\circ}$ , (c)  $+90^{\circ}$ , (d)  $-45^{\circ}$ , and (e)  $-90^{\circ}$**

The initial load was 5 W and, after approximately 15 minutes, the thermocouples showed stationary values. If it had happened, the thermal load was increased by 5 W. The load increment was made until the maximum temperature of the heat pipe reached the critical temperature,  $150\text{ }^{\circ}\text{C}$ , where the melting of the materials could happen. Data was acquired every 5 seconds, recorded in the desktop by the software Agilent<sup>TM</sup> Benchlink Data Logger 3.

## Data reduction

The thermal performance of the heat pipes was analyzed and compared by the operating temperature,  $T_{op}$ , and the thermal resistance,  $R_{th}$ . The analyzed operating temperature is the temperature of the adiabatic region,  $T_{adiab}$ . The thermal resistance,  $R_{th}$ , of the heat pipes can be defined as the difficulty of the device to carry heat and can be calculated by:

$$R_{th} = \frac{T_{evap} - T_{cond}}{q_{in}} \quad (1)$$

where  $q_{in}$  is the input heat on the heat pipe,  $T_{evap}$  and  $T_{cond}$  are the average wall temperature of the evaporator and the condenser, respectively.

The experimental uncertainties are associated with the *K*-type thermocouples, the data logger, and the power supply unit. The error propagation method described by [24] was used to determine the uncertainty of the electrical power measurement obtained from the electrical resistors and to determine the uncertainties of the thermal resistance of the heat pipes. The uncertainties of the measured data were estimated for the thermocouple temperatures and the input power, considering the accuracy of the *K*-type thermocouples of  $\pm 2.2^\circ\text{C}$ , the voltage of  $0.35\% + 20 \text{ mV}$  and the current of  $0.35\% + 20 \text{ mA}$ . The uncertainties were evaluated as rectangle type for all measures because the maximum and minimum values of variation of each equipment used are known. The determination of the combined uncertainty was defined as the correlated type, based on the nature of the data acquired through the experiment. The experimental temperature uncertainty is estimated to be approximately  $\pm 1.27^\circ\text{C}$  and a thermal load was  $\pm 1\%$ . They are shown with the obtained results.

## Results and discussion

The experimental results regarding the thermal performance of the heat pipes are presented considering 5 positions:  $0^\circ$ ,  $+45^\circ$ ,  $+90^\circ$ ,  $-45^\circ$ , and  $-90^\circ$ , in relation to the horizontal. The experimental tests were repeated three times and the errors were compared taking into account the difference between the mean values were less than  $0.5^\circ\text{C}$ . Tests were performed under different heat loads varying from 5-50 W or a heat flux from  $0.21\text{-}2.10 \text{ W/cm}^2$ .

Figure 7 shows the temperature distribution as a function of time for the heat pipe with microgrooves of Type 1 in the different operating positions. For the horizontal, the maximum dissipated power was 40 W. For the  $-45^\circ$  and  $-90^\circ$  in relation to the horizontal (evaporator above condenser), the maximum power was 15 W, while for the  $+45^\circ$  and  $+90^\circ$  (evaporator under condenser) the maximum dissipated power was 45 W. The maximum heat load was achieved for the best operating condition where the condenser is above evaporator in which the gravity action joins the capillary pumping in order to maintain the evaporation into the evaporator. The minimum heat load was achieved in adverse condition where the gravity action is contrary to the capillary pumping and the capillary limit was achieved and the heat pipe stopped to work for higher heat loads.

The experimental results of the temperature distribution of the heat pipes with microgrooves Type 2 and Type 3 are very similar to the thermal behavior of Type 1 heat pipe, then all the temperatures increase with the rise of the dissipated power, in positions against to the gravity the heat pipes supported 15 W and in the other positions they had a satisfactory performance. The difference of the heat pipes Type 2 and Type 3 and the heat pipe Type 1 is only the magnitude of the values that influence in the maximum dissipated power. Table 3 shows the operating temperature for the three types of heat pipes in the horizontal position, which illustrate this difference in the magnitude of the values.

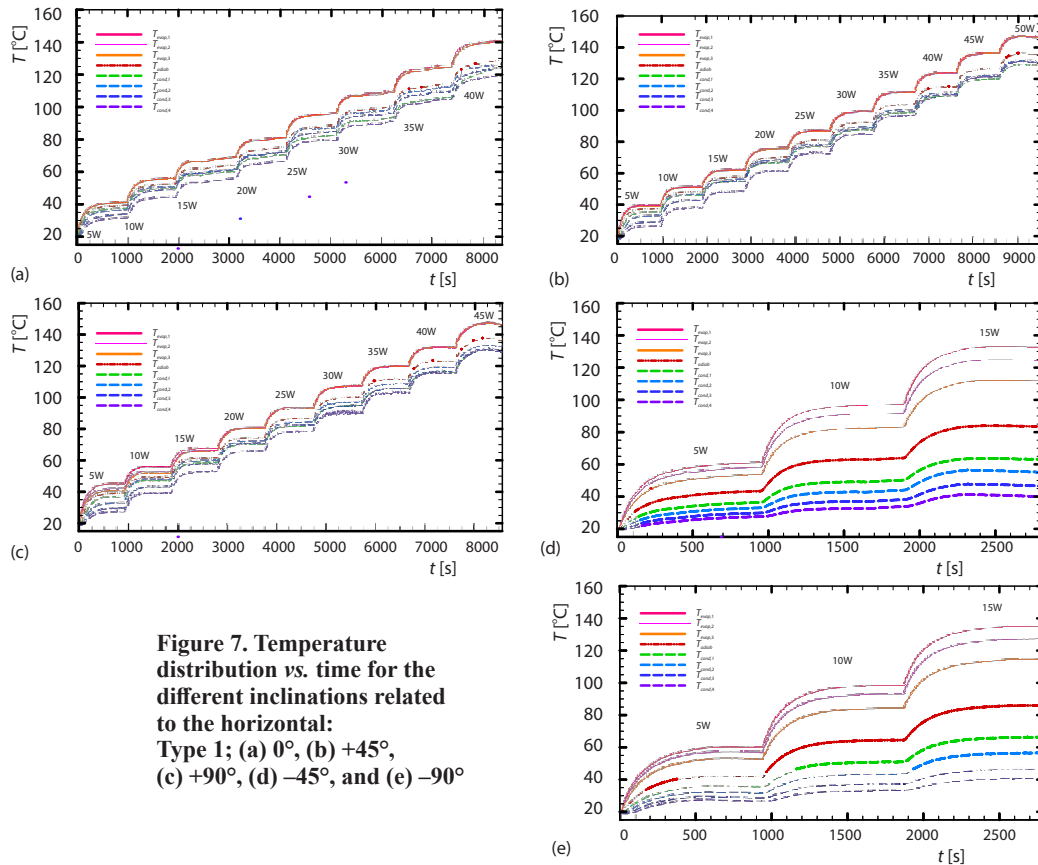


**Figure 7. Temperature distribution vs. time for the different inclinations related to the horizontal: Type 1; (a) 0°, (b) +45°, (c) +90°, (d) -45°, and (e) -90°**

**Table 3. Operating temperature of heat pipes in the horizontal position**

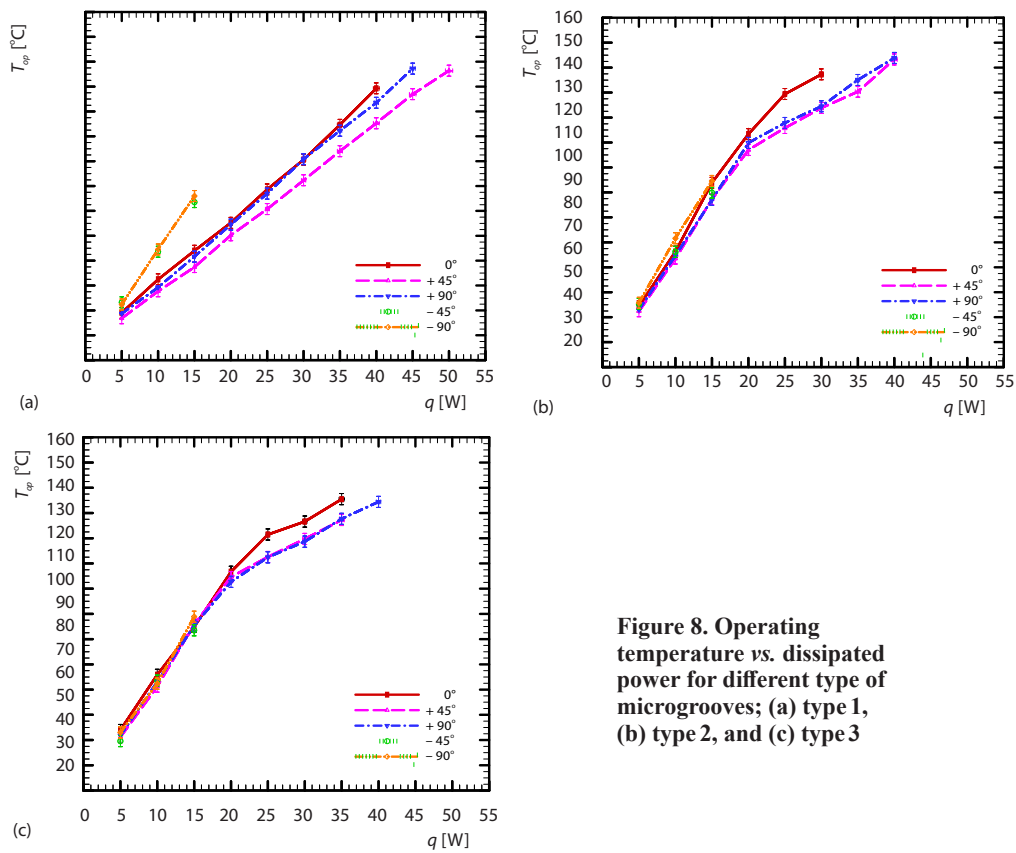
Heat load [W]	Heat pipe		
	Type 1	Type 2	Type 3
5	39.0	44.3	44.0
10	52.4	66.3	65.9
15	63.9	93.9	84.9
20	75.2	113.4	106.7
25	88.6	129.4	121.5
30	100.6	137.3	126.6
35	114.6	–	135.5
40	129.2	–	–

Figure 8 shows the behavior of the operating temperature as a function of the dissipated power parameterized in the operating position of the different microgrooves heat pipes. It may be noted that as the dissipated power increases, the operating temperature also increases. The reason for this behavior is the operating temperature dependence on the intern pressure of the heat pipe, which varies with the dissipated power in the evaporator. According to Ku [25],

in most of the two-phase capillary pumping systems, the changes of pressure and temperature are extremely small. These changes along a saturation-line may be approximated using the Clausius-Clapeyron equation:

$$\frac{dp}{dT} \Big|_{T_{\text{sat}}} \frac{h_{\text{lv}}}{T_{\text{sat,lv}}} \quad (2)$$

where  $h_{\text{lv}}$  is the latent heat of vaporization,  $T_{\text{sat}}$  – the saturation temperature. Therefore, the main characteristic of a heat pipe is its strong dependence of the operating temperature on the input heat.



**Figure 8. Operating temperature vs. dissipated power for different type of microgrooves; (a) type 1, (b) type 2, and (c) type 3**

Figure 9 illustrates the behavior of the thermal resistance as a function of power dissipation considering the different operating positions for the three types of microgrooves. In the most cases, the thermal resistance decrease with the increasing heat dissipation in the evaporator. The thermal resistances obtained by the fabricated heat pipe are acceptable since the values are similar to the heat pipes made by other technique of fabrication [26]. The heat pipes in  $+45^\circ$  and  $+90^\circ$  to the horizontal presented the best thermal performance, due to lower thermal resistance. The reason is that the gravity helps to improve the capillarity. For the  $-45^\circ$  and  $-90^\circ$  to the horizontal, the capillarity has to work against gravity, which causes the high thermal resistance.

The experimental results of this study were satisfactory since all the types of axial microgrooves worked satisfactorily as a capillary structure for heat pipes. So, the wire-EDM,

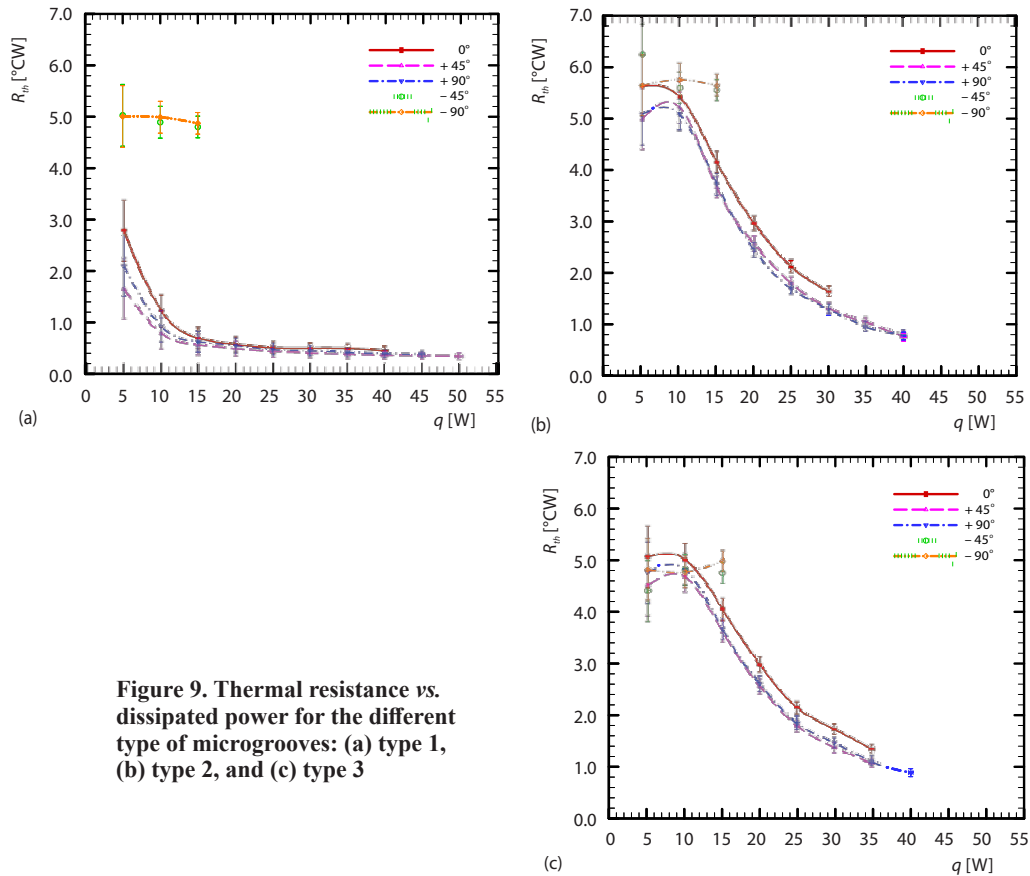


**Figure 9. Thermal resistance vs. dissipated power for the different type of microgrooves: (a) type 1, (b) type 2, and (c) type 3**

can be effectively used as manufacturing technology of microgrooves. Due to the lower thermal resistance and operating temperature, the microgrooves of Type 1 ( $\delta = 30 \mu\text{m}$ ,  $w = 35 \mu\text{m}$ ,  $w_f = 35 \mu\text{m}$ , and  $N = 32$ ) presented the better thermal performance when compared with the others types of microgrooves. The lower the curvature radius the higher the capillary pumping, assuming that the capillary radius in this work is equivalent to microgroove depth. As a result, when the capillary pumping is effective the evaporation can be better controlled and the thermal resistance is low due to the low temperature difference between the evaporator and condenser region. This phenomenon is observed in heat pipe Type 1 and that is why it presented the best results for thermal resistances. It can also be noticed that the heat pipe Type 3 has the same microgroove depth (30 m), however the number of microgrooves was lower and the thermal resistance through the transversal area due to the solid increased the thermal resistance.

### Conclusions

In this work, heat pipes with three different types of axial microgrooves were manufactured and experimentally tested. These capillary structures were fabricated by wire-EDM. The microgrooves had an average diameter of  $220 \mu\text{m}$ . The heat pipes were 200 mm long, their inner and outer diameters were 6.20 mm and 9.45 mm, respectively, and the working fluid was water. Experimental tests were performed under 5 different inclinations ( $0^\circ$ ,  $+45^\circ$ ,  $+90^\circ$ ,  $-45^\circ$ , and  $-90^\circ$ ) related to the horizontal, under different heat loads (from 5-50 W or a heat flux from

0.21-2.10 W/cm<sup>2</sup>). The experimental results showed that the axial microgrooves manufactured by the wire-EDM process worked satisfactorily in all analyzed cases and microgrooves of Type 1 ( $\delta = 30 \mu\text{m}$ ,  $w = 35 \mu\text{m}$ ,  $w_f = 35 \mu\text{m}$ , and  $N = 32$ ) showed a better thermal performance when compared with the others.

Although, all the heat pipes have presented satisfactory thermal performance, the thermal resistances were primordial to affirm that heat pipe Type 1 was the best configuration, because the microgrooves depth of this passive device was lower and the number of microgrooves was higher in comparison the other types (2 and 3). According to the results of the thermal resistances, it is suggested that the microgroove depth should be decreased (lower than 30  $\mu\text{m}$ ), the number of microgrooves should be increased (higher than 32) and the tube thickness should be smaller since the pressure into the heat pipe is not high.

### Acknowledgment

Acknowledgments are provided to the Capes, the CNPq, the PROPPG/UTFPR, the DIRPPG/UTFPR, the PPGEM/UTFPR/*Campus* Ponta Grossa, and the DAMEC/UTFPR/*Campus* Ponta Grossa.

### Nomenclature

$h_{lv}$  – latent heat of vaporization, [Jkg<sup>-1</sup>]  
 $N$  – number of microgrooves, [–]  
 $p$  – pressure, [Pa]  
 $q_{in}$  – input heat, [W]  
 $R_{th}$  – thermal resistance, [°CW<sup>-1</sup>]  
 $T$  – temperature, [°C]  
 $t$  – time, [s]  
 $w$  – microgroove width [m]  
 $w_f$  – microgroove thickness [m]

#### Greek symbols

$\delta$  – microgroove depth, [m]

$\phi$  – wire diameter from the wire-EDM process, [m]  
 $v$  – specific volume, [m<sup>3</sup>kg<sup>-1</sup>]

#### Subscripts

adiab – adiabatic section  
 cond – condenser  
 evap – evaporator  
 l – liquid phase  
 in – input  
 op – operating  
 sat – saturation  
 v – vapor phase

### References

- [1] Krambeck, L., et al., Thermal Performance Evaluation of Different Passive Devices for Electronics Cooling, *Thermal Science*, 23 (2017), 2B, pp. 1151-1160
- [2] Faghri, A., Heat Pipes: Review, Opportunities and Challenges, *Frontiers in Heat Pipes*, 5 (2014), Apr., pp. 1-48
- [3] Reay, D. A., et al., *Heat Pipe: Theory, Design and Applications*, Butterworth-Heinemann, Amsterdam, Netherland, 2014
- [4] Peterson, G. P., An Introduction Heat Pipes: Modelling, Testing and Applications, in: *Thermal Management of Microelectronic and Electronic System Series*, Wiley-Interscience, New York, USA, 1994
- [5] Groll, M., Rosler, S., Operation Principles and Performance of Heat Pipes and Closed Two-Phase Thermosyphons, *Journal of Non-Equilibrium Thermodynamics*, 17 (1992), 2, pp. 091-151
- [6] Chi, S. W., *Heat Pipe Theory and Practice: A Sourcebook*, Hemisphere Publishing Corporation, Washington, USA, 1976
- [7] Krambeck, L., et al., Experimental Research of Capillary Structure Technologies for Heat Pipes, *Proceedings*, 24<sup>th</sup> ABCM International Congress of Mechanical Engineering, Curitiba, Brazil, 2017
- [8] Krambeck, L., et al., Heat Pipe with Axial Microgrooves Fabricated by Wire Electrical Discharge Machining (Wire-EDM), *Proceedings*, 9<sup>th</sup> World Conference on Experimental Heat Transfer, Fluid Mechanics and Thermodynamics, Foz do Iguacu, Brazil, 2017
- [9] Tang, Y., et al., Experimental Study of Oil-Filled High-Speed Spin Forming Micro-Groove Fin-Inside Tubes, *International Journal of Machine Tools and Manufacture*, 47 (2006), 7-8, pp. 1059-1068
- [10] Wang, X., et al., Investigation into Performance of a Heat Pipe with Micro Grooves Fabricated by Extrusion-Ploughing Process, *Energy Conversion and Management*, 50 (2009), 5, pp. 1384-1388

- [11] Chen, S. W., *et al.*, Experimental Investigation and Visualization on Capillary and Boiling Limits of Micro-Grooves Made by Different Processes, *Sensors and Actuators A*, 139 (2007), 1-2, pp. 78-87
- [12] Yang, X., *et al.*, Recent Developments of Lightweight, High Performance Heat Pipes, *Applied Thermal Engineering*, 33-34 (2012), Feb., pp. 1-14
- [13] Nishida, F. B., Development of Heat Pipes with Microgrooves Fabricated by Wire Electrical Discharge Machining (in Portuguese), M. Sc. thesis, Dissertação de Mestrado em Engenharia Mecânica, Universidade Tecnológica Federal do Paraná, Ponta Grossa, Brazil, 2016
- [14] Li, Y., *et al.*, Forming Method of Axial Micro Grooves Inside Copper Heat Pipe, *Transactions of Non-Ferrous Metals Society of China*, 18 (2008), 5, pp. 1229-1233
- [15] Chang, Y. W., *et al.*, Heat Pipe for Cooling of Electronic Equipment, *Energy Conversion and Management*, 49 (2008), 11, pp. 3398-3404
- [16] Tang, Y., *et al.*, Experimental Investigation into the Performance of Heat Pipe with Micro Grooves Fabricated by Extrusion-Ploughing Process, *Energy Conversion and Management*, 51 (2010), 10, pp. 1849-1854
- [17] Tang, Y., *et al.*, Effect of Fabrication Parameters on Capillary Performance of Composite Wicks for Two-Phase Heat Transfer Devices, *Energy Conversion and Management*, 66 (2013), Feb., pp. 66-76
- [18] \*\*\*, Vancouver Wire EDM, [http://www.vancouverwireedm.com/Wire\\_EDM\\_Tips\\_For\\_Machinists.htm](http://www.vancouverwireedm.com/Wire_EDM_Tips_For_Machinists.htm)
- [19] Sommer, C., *Non-Traditional Machining Handbook*, Advance Publishing Inc., Houston, Tex., USA, 2000
- [20] Bobbili, R., *et al.*, Modelling and Analysis of Material Removal Rate and Surface Roughness in Wire-Cut EDM of Armour Materials, *Engineering Science and Technology*, 18 (2015), 4, pp. 664-668
- [21] Krambeck, L., Experimental Investigation of Wire Mesh Thermal Performance in Heat Pipes (in Portuguese), Ph. D. thesis, Trabalho de Conclusão de Curso de Graduação em Engenharia Mecânica, Universidade Tecnológica Federal do Paraná, Ponta Grossa, BRA, 2016
- [22] Santos, P. H. D., *et al.*, Modelling and Experimental Tests of a Copper Thermosyphon, *Acta Scientiarum, Technology*, 39 (2017), 1, pp. 59-68
- [23] \*\*\*, American Society of Heating, Refrigerating and Air-Conditioning Engineers, ASHARE Handbook: Fundamentals, ASHARE, New York, USA, 2017
- [24] Holman, J. P., *Experimental Methods for Engineers*, McGraw-Hill, New York, USA, 2011
- [25] Ku, J., Operating Characteristics of Loop Heat Pipes, *Proceedings*, 29<sup>th</sup> International Conference on Environmental System, Denver, Col., USA, 1999
- [26] Hu, Y., *et al.*, Thermal Performance Enhancement of Grooved Heat pipes with Inner Surface Treatment, *International Journal of Heat and Mass Transfer*, 67 (2013), Dec., pp. 416-419